A Time-Domain Twice Expansion Method for Wave Interaction with a Body of Large Amplitude Motion

Bin Teng, Ruijia Jin
State Key Laboratory of Coastal and Offshore Engineering
Dalian University of Technology
Dalian, 116024, Liaoning, China
E-mail: bteng@dlut.edu.cn

1. Introduction

Deep water structures are usually positioned in sea by mooring lines, which perform strong nonlinearity. The structure system usually has a very low natural frequency, and can be inspired lager reciprocating drift motion by nonlinear wave force at low frequency.

To deal with the problem due to mooring nonlinearity, Sarkar and Eatock Taylor (1998, 2001) proposed a two-scale perturbation method to investigate the interactions of nonlinear mooring stiffness and wave hydrodynamics, and established a frequency domain perturbation method for this problem.

The nonlinear problem is more widely studied in the time domain, and coupling analysis must be carried out for wave interaction with floater and mooring system. As the total time domain coupling analysis is complex and tremendous, hydrodynamic load is often computed by a perturbation expansion method (as Yang et al (2012)), or by Cummins method based on the frequency domain perturbation expansion (as Kim et al (2013)).

Perturbation method is powerful when body motion is not very large. However, in deep water the floater may oscillate with an amplitude larger than wave lengths. At this condition, the traditional perturbation expansion is obviously not correct. The most obvious disadvantages of the present perturbation method are that the phase change of the wave load due to body motion and the change of the encountering frequency of incident waves are unable to be considered. To solve those problems, a time domain twice expansion method is proposed in this study. The displacement of floater motion is divided into two part: one is a large amplitude motion with low frequency, and the other is an oscillation about the low frequency motion at higher frequency. The large amplitude motion at low frequency is obtained by numerical filtering of body response with progress of the simulation. This position is called as the instantaneous mean position. The smaller amplitude motion about the mean position is computed by perturbation expansion method. Thus, it can be guaranteed that the perturbation expansion factor is always smaller.

The numerical filtering is implemented by a wavelet transform method in this study, and a HOBEM is applied to calculate the wave field at each time step. At each time step, the overall body and free surface meshes vary with the low frequency movement, but the relative location of the computational grids is invariant. Recursive interpolation is used to get the physical values for those nodes inside the free surface mesh, and Taylor series expansion is used for the boundary nodes after the body and the mesh have translated to a new position. At the new position, computation is similar with that for wave interaction with a body moving in a steady current.

2. Definition of coordinate systems and decomposition of body motion

To describe the motion of a floating body, three coordinate systems (**Fig. 1**) are defined. The first is an earth-fixed coordinate system $Oxyz$ at the initial equilibrium position of the body, the second is an instantaneous mean coordinate system $\overline{Oxyz}$ translating horizontal with the body at low frequency and the third is a body-fixed coordinate system $O'x'y'z'$. The origins of the coordinate systems $Oxyz$ and $\overline{Oxyz}$ are at the still water surface, and the z and the $\overline{z}$ axes measure vertically upward.

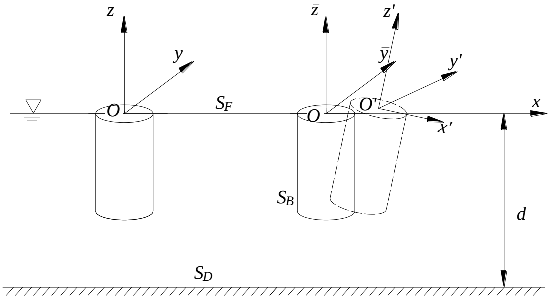

Fig. 1 Definition sketch of coordinate systems

When the body is undergoing a large drift motion, the second coordinate system will be far away from the first one. For any point on the body, the coordinate vector X in the earth-fixed coordinate system can be represented by the coordinate vector $\boldsymbol{X}'$ in the body-fixed coordinate system and it motion components in the following relationship:

$$\boldsymbol{X} = \boldsymbol{X}'(t) + \Xi(t) \tag{1}$$

and

$$\Xi(t) = \bar{\boldsymbol{X}}(t) + (\boldsymbol{\xi} + \boldsymbol{\alpha} \times (\boldsymbol{X}'(t) - \boldsymbol{X}'_0(t))) \tag{2}$$

where $\overline{\mathbf{X}}(t)$ is the displacement of the instantaneous mean coordinate system $\overline{Oxyz}$ with only the horizontal translation, $\boldsymbol{X}'_{\mathbf{0}}$ is the body rotation center, ξ and $\boldsymbol{\alpha}$ are the body translation and rotation components relative to the instantaneous mean coordinate system. $\overline{\mathbf{X}}(t)$ will be obtained by a numerical filtering method with the simulation of body response, which will be introduced in the next section.

Following the Stokes expansion procedure, we expand the body motion relative to the instantaneous mean position $\overline{\mathbf{X}}(t)$ into perturbation series as follows:

$$\xi(t) = \varepsilon\xi^{(1)}(\bar{\mathbf{X}},t) + \varepsilon^2\xi^{(2)}(\bar{\mathbf{X}},t) + \cdots \tag{3}$$

$$\alpha(t) = \varepsilon\alpha^{(1)}(\bar{\mathbf{X}},t) + \varepsilon^2\alpha^{(2)}(\bar{\mathbf{X}},t) + \cdots \tag{4}$$

The superscripts (1) and (2) indicate separately the wave components at the first-order and the second-order of ε respectively.

In the same way, the velocity potential ϕ and wave elevation η can be expanded as

$$\phi(\bar{\mathbf{X}},t) = \varepsilon\phi^{(1)}(\bar{\mathbf{X}},t) + \varepsilon^2\phi^{(1)}(\bar{\mathbf{X}},t) + \cdots \tag{5}$$

$$\eta(\bar{\mathbf{X}},t) = \varepsilon\eta^{(1)}(\bar{\mathbf{X}},t) + \varepsilon^2\eta^{(1)}(\bar{\mathbf{X}},t) + \cdots \tag{6}$$

at the instantaneous mean positions by the parameter ε.

Then the Stokes perturbation expansions are substituted into the Laplace equation and the corresponding boundary conditions are expanded about the still water surface and the instantaneous mean body surface. The boundary value problems at the order of ε and ε^2 in the perturbation expansions can be established.

As the instantaneous mean coordinate system moves with very low frequency, the acceleration of the system is a higher order term of ε, and the system can be approximated as an inertial system. Thus, the governing equation, boundary conditions, wave force and motion equation are the same as in the earth-fixed coordinate system, and computation can be done in the same way as for a steady moving body in waves (Liu et al, 2012).

3. Computation of mean position and mesh translation

Deep water moored platforms may move to far distances from their initial positions. For accurate computation, an instantaneous mean position is needed to get and carries out perturbation expansion about the position. According to the time sequence of the motion response simulated, we use a wavelet transform to get the mean position of the motion response (Chritopher and Gilbert, 1998).

Assuming that the time sequence of the motion response is $\Xi(t)$ (0, t), and is progressing with the time, the continuous wavelet transform of a discrete sequence is defined as the convolution of Ξ with a scaled and translated version of $\Psi_0(\eta)$. By the convolution theorem, the wavelet transform is the inverse Fourier transform of the product

$$WT(s,t) = \sum_{n=0}^{N-1} \hat{\Xi}\hat{\psi}^*(s\omega_k)e^{\mathrm{i}\omega_k n\Delta t} \tag{7}$$

In the actual application of wavelet transform, the selection of mother wavelet function has a crucial impact on the analysis results. For the same problem, the analysis results may differ very much if different mother wavelets are chosen. In the present analysis, the instantaneous mean displacement $\overline{\mathbf{X}}(t)$ is not needed to be unique, but only the total displacement $\Xi(t)$ to be needed unique. The study in this paper is based on the Morlet wavelet as the mother wavelet. Since the wavelet transform is a band pass filter with a known response function, it is possible to reconstruct the original time series using either deconvolution or the inverse filter.

$$\Xi(t) = \frac{\delta j \Delta t^{1/2}}{C_\delta \psi_0(0)} \sum_{j=0}^{J} \frac{\mathrm{Re}\{WT(s_j,t)\}}{s_j^{1/2}} \tag{8}$$

where C_δ is the reconstruct coefficient. For the mean position of the displacement time series, there is no need to evaluate all the scales. The small scales just should be left out and the expected results $(\bar{X}_x(t), \bar{X}_y(t))$ will be obtained.

When the Morlet wavelet is selected as the mother wavelet, the value of reconstruct coefficients C_δ and $\psi_0(0)$ will be 0.776 and $\pi^{-1/4}$.

Let the body surface mesh and free surface mesh drift horizontally with the body mean displacement. When the meshes moving to new mean positions, the right-hand side of integration equation, i.e. the known quantities, would be evaluated based on the values at the last time step. The wave elevation also needs to conduct recursive calculation by the free surface conditions. Due to the meshes moving as a whole, the grid shape will not change, so that the velocity potentials and wave elevations at the new time step can be determined by interpolation for those points inside the free surface meshes or by using Taylor expansion for those points at the boundaries of the free surface mesh as

$$f_{t+\Delta t}^{(1)}(x,y) = f_t^{(1)}(x_0,y_0) + \frac{\partial f_t^{(1)}}{\partial x}\nabla x + \frac{\partial f_t^{(1)}}{\partial y}\nabla y$$

$$f_{t+\Delta t}^{(2)}(x,y) = f_t^{(2)}(x_0,y_0) + \frac{1}{2}\frac{\partial^2 f_t^{(1)}}{\partial x^2}\nabla x^2 + \frac{1}{2}\frac{\partial^2 f_t^{(1)}}{\partial y^2}\nabla y^2 + \frac{\partial^2 f_t^{(1)}}{\partial x \partial y}\nabla x \nabla y + \frac{\partial f_t^{(2)}}{\partial x}\nabla x + \frac{\partial f_t^{(2)}}{\partial y}\nabla y \tag{8}$$

where f indicates scattered potential ϕ_s or scattered wave evaluation η_s at the free surface.

4. Example analyses

To validate the present method, a forced moving truncated cylinder in monochromatic waves and a free moving truncated cylinders in bichromatic waves are considered.

4.1. Forced motion in waves

The first evaluation is about forced oscillation of a truncated cylinder in monochromatic waves. The cylinder has a radius of 1m and a draft of 0.5m in a water depth of 1.5m. The incident waves have an amplitude of A=0.1m with a frequency of ω=2.98rad/s (k=0.6m^{-1}), and propagating in the x-direction.

The cylinder is under a forced dual-frequency motion:

$$\Xi_x = A_1 \sin(\omega_1 t + \varphi_1) + A_2 \sin(\omega_2 t + \varphi_2) \qquad (9)$$

where A_1=0.4m, ω_1=2.98rad/s (k_1=1.0m^{-1}) and φ_1=45° are the amplitude, frequency and initial phase of the higher-frequency small-amplitude motion, and A_2=2.0m, ω_2=0.19rad/s (k_2=0.05m^{-1}) and φ_2=0° are the amplitude, frequency and initial phase of the lower-frequency large-amplitude motion.

The wave exciting force on the moving body is decomposed into the components due to the incident potential and the scattered potential, which are defined as F_w and F_s. Fig. 2 and 3 how the comparison of the first order and the second order forces by the present method with the original expanded method in the earth-fixed coordinate system. From Fig. 2, it can be seen that there exists obvious phase difference between the incident wave forces from the two methods. When body mean position is positive, the phase of the incident wave force obtained by the present method is later than that by the original one, as the incident waves reach the present body position later than the original position. In turn, when the mean position is negative, the phase of incident wave force obtained by the present method is earlier than that by the original method. This conclusion is consistent with the actual situation. While to the wave force generated by the scattered potential, the phases of wave forces obtained by the two methods are the same, but the envelop shapes are different. The present results fluctuate around the original ones, and the oscillating period is equal to the period of the low frequency forced motion. The difference is from the motion velocity of the instantaneous mean position which is neglected in the original method.

The total force is the summation of the two parts. It was observed the total forces from the two methods are quite different. The amplitude of the total force from the original method is steady and uniform, but the force amplitude from the present method oscillating with the time. When body moves to a position where incident wave force and scattered wave force have the same phase, the total force from the present method are much bigger than that from the original ones. Oppositely, the present results are smaller than the original ones.

The second-order total wave force contains more complex components. There are more differences between the present and the original methods.

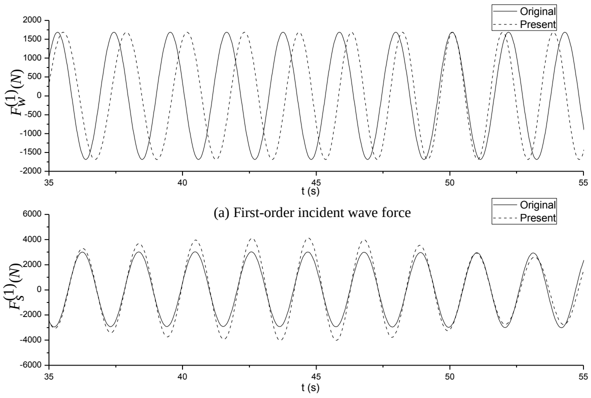

(a) First-order incident wave force

(a) First-order scattered wave force

Fig. 2 Comparison of the first-order wave force

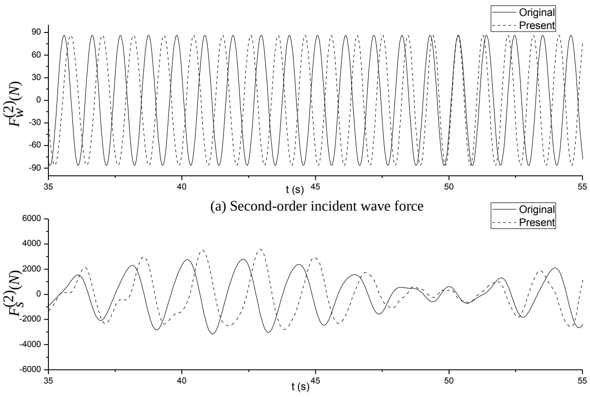

(a) Second-order incident wave force

(b) Second-order scattered wave force

Fig. 3 Comparison of the second-order wave force

4.2. Free motion in waves

It is seen that the present method gets quite different results for a body undergoing a large amplitude motion from that by the original method. Through analysis and comparison, it is believed that the present method is more reasonable and more suitable for realistic conditions.

This example shows the analysis for a free moving truncated cylinder moored by linear elastic constrain under the action of bichromatic waves. The cylinder has a radius of 1.0m and a draft of 3.0m in a water depth of 10.0m. A linear spring is arranged in the surge direction to constrain the motion of the cylinder and the stiffness of the spring is 4×10^2N/m. The natural vibration frequency of the system is about 0.151rad/s. The parameters of the bichromatic waves are shown in

Tab. 1 as follow.

Tab. 1 Parameters of the bichromatic waves

Items	Wave Amplitude(m)		Wave Frequency(rad/s)		Wave Direction(°)	
	A_1	A_2	ω_1	ω_2	θ_1	θ_2
Value	0.20	0.18	2.20	2.40	0.00	0.00

From the above table, we can see that the difference frequency of the bichromatic waves is 0.2rad/s that is in the same order of the natural frequency of the system.

Fig. 4 shows the comparison of the wave forces from the present and the original methods. **Fig. 5** shows the comparison of the surge displacements from the present and the original methods. From Figs. 4 and 5, it can be seen that the first order wave forces and the body motion from the two methods are almost the same, as the total surge displacement is much less than the wave lengths. The second-order wave forces from the two method exist some differences, and difference between the second order displacements is very obvious. It can also be seen that the second order displacement is much larger than the first order displacement as the difference frequency of the bichromatic waves is close to the natural frequency of the moored cylinder.

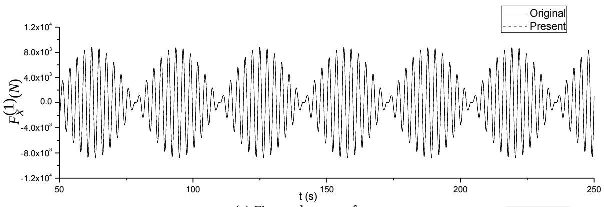

(a) First-order wave force

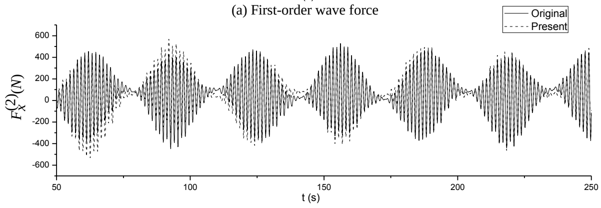

(b) Second-order wave force

Fig. 4 Comparison of wave forces

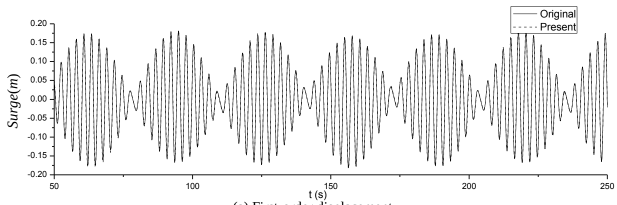

(a) First-order displacement

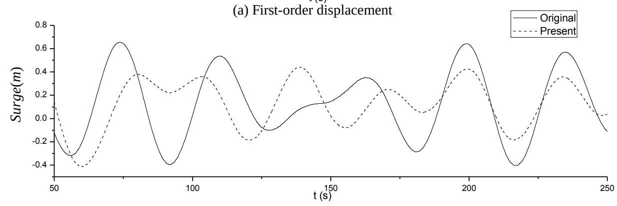

(a) Second-order displacement

Fig. 5 Comparison of surge displacement

5. Conclusion

A twice expansion method in the time domain is developed in this study. The present method firstly gets the instantaneous mean position with the simulation by filtering the total motion response, and then carries out perturbation expansion about the mean position to assure the perturbation expansion factor is always smaller. The present method can deal with the problems of the phase change of incident wave action with the body motion and the change of encountering frequency of the incident waves with body moving velocity.

Two numerical examples are carried out, and comparisons are made between the present and the original methods. One is the forced motion of a truncated cylinder with dual-frequencies in a monochromatic waves, and the other is the free motion of a moored truncated cylinder in a bichromatic waves. Comparisons show that when the displacement of the body motion is large, both the first order and the second order force are different for the two methods, and when the displacements are smaller comparing to wave lengths the first order forces and displacements are almost the same, but the second order responses still have obvious difference.

Acknowledgements

This work was supported by the National Natural Science Foundation of China (Grant Nos. 51379032, 51490672), and the National Basic Research Program of China (“973” Program) (Grant No. 2011CB013703).

REFERENCES

[1] Kim BW, Hong GS, Kim JH, Hong SY, 2013, Comparison of linear spring and nonlinear FEM methods in dynamic coupled analysis of floating structure and mooring system, *Journal of Fluids and Structures*, 42, 205-227.

[2] Liu Z, Teng B, Ning DZ, Gou Y, 2010, Wave-current interactions with three-dimensional floating bodies, *Journal of Hydrodynamics*, 22(2), 229-240.

[3] Sarker A, Eatock Taylor R, 1998, Low-frequency responses of non-linearly moored vessels in random waves: development of a two-scale perturbation method, *Applied Ocean Research*, 20, 225-236.

[4] Sarker A, Eatock Taylor R, 2001, Low-frequency responses of non-linearly moored vessels in random waves: coupled surge, pitch and heave motions, *Journal of Fluids and Structures*, 15, 133-150.

[5] Chritopher T, Gilbert CP, 1998, A practical guide to wavelet analysis, *Bulletin of American Meteorological Society*, 79(1), 64-78.

[6] Yang MD, Teng B, Ning DZ, Shi ZM, 2012, Coupled dynamic analysis for wave interaction with a truss spar and its mooring linear/riser system in time domain, *Ocean Eng*, 39, 72-87.